Electronic entropy change in Ni-doped FeRh

N. Pérez [a, *], A. Chirkova [a, b], K.P. Skokov [b], T.G. Woodcock [a], O. Gutfleisch [b], N.V. Baranov [c, d], K. Nielsch [a, e], G. Schierning [a]

[a] IFW Dresden, Institute for Metallic Materials, Helmholtzstrasse 20, Dresden, 01069, Germany
[b] Materials Science, TU Darmstadt, Darmstadt, 64287, Germany
[c] Institute of Natural Sciences and Mathematics, Ural Federal University, Yekaterinburg, 620083, Russia
[d] M. N. Miheev Institute of Metal Physics, Ural Branch of Russian Academy of Sciences, Yekaterinburg, 620108, Russia
[e] TU Dresden, Institute of Materials Science, 01062, Dresden, Germany

ARTICLE INFO

ABSTRACT

The net entropy change corresponding to the free charge carriers in a Ni-doped FeRh bulk polycrystal was experimentally evaluated in a single sample using low-temperature heat capacity experiments with applied magnetic field and using Seebeck effect and Hall coefficient measurements at high temperatures across the first-order phase transition. From the heat capacity data, a value for the electronic entropy change $\Delta S_{el} \approx 8.9$ J kg^{-1}K^{-1} was extracted. The analysis of the Seebeck coefficient allows tracing the change of the electronic entropy jump with applied magnetic field directly across the transition. The difference in electronic entropy contribution obtained is as high as 10% from 0.1 to 6 T.

© 2019 Elsevier Ltd. All rights reserved.

1. Introduction

The determination of entropy changes in solids at phase transitions of different kinds is of major relevance for understanding fundamental phenomena in materials and a source of information for their design and optimization for applied purposes. Typical examples can be found in the phase transitions of magnetocaloric materials [1], shape memory alloys [2], or piezoelectrics/ferro-electrics [3]. The total entropy change is the result of several contributions coming from the ion lattice, magnetization changes, electrical polarization changes, or conduction electrons. Evaluating the different contributions is necessary to understand the transition processes. Particularly, the entropy associated with the conduction electrons is crucial in the understanding of correlated electron systems [4], including magnetic [5], semiconducting [6], and superconducting [7] materials. In that context, the experimental determination of thermodynamical quantities in low-dimensional systems is a matter of current interest [8].

Here, we investigate the first-order metamagnetic transition in Ni-doped α-FeRh. The transition from a low temperature antiferromagnetic (AF) phase to a high-temperature ferromagnetic (FM) phase [9–11] shows a large entropy change reaching $\Delta S \approx 16$ J

kg^{-1}K^{-1} [12] and a change in lattice parameter [13,14]. Different works attributed the origin of the transition to processes involving conduction electrons [9,10], magnetic instability associated with magnon modes [15], or lattice instability [16]. The different entropy contributions to the phase transition were evaluated either theoretically [17] or experimentally using a set of proxy thin film samples (in the terminology used by Cooke et al.) for the different magnetically ordered states [18]. Recent theoretical studies addressed the importance of changes in electronic structure at the phase transition [19], and an additional barrierless martensitic transition was predicted to occur below about 90 K [20].

In this work, we studied the electronic part of that singular phase transition in a Ni-doped FeRh polycrystal using low-temperature heat capacity. In addition, using Seebeck and Hall coefficient measurements, the evolution of the entropy change with applied field was evaluated. The differences between calorimetric and electronic transport approaches are discussed. The Hall coefficient measurements indicate a complex magnetic behavior in the AF phase before the transition and show a small step at around 90 K which could be related to the recently theoretically predicted existence of an additional transition at approximately 90 K. The latter would need further investigation.

---

2. Evaluation of the electronic entropy

In the usual experimental approach, heat capacity measurements at low temperatures are performed and interpreted making use of the approximated series expansion $C_p = \gamma T + \sum_{i=3,5,7} \beta_i T^i + C_m$·, where γ is the electronic specific heat coefficient, β_i are the lattice specific heat coefficients, and C_m is the magnetic contribution to the specific heat. However, in the presence of a phase transition at higher temperatures, typically several samples of different compositions and different magnetic ordering at low temperature need to be studied to experimentally determine difference in γ between the differently magnetically ordered states [9,11,18]. In our approach, low-temperature C_p was measured in the same sample for the different magnetically ordered states forcing the metamagnetic transition with an applied magnetic field of sufficient intensity. The Seebeck coefficient α inherently contains information about the entropy of the charge carriers, as derived by Ioffe [21] and recently revised by Goupil et al. [22], both from thermodynamical arguments. A simplified derivation can be performed for isotropic materials using the definition of the Peltier coefficient, $\Pi = Q/(eN_t)$, as the heat Q per transported carrier N_t and Onsager's reciprocal relation, $\Pi = \alpha \cdot T$. Both relations lead in a simple way to the formal expression that relates α and the entropy associated with the effectively transported charge carriers, $\alpha = Q/(TeN_t) = S_t/(eN_t)$. The value of the elemental charge e is conventionally taken with sign depending on the type of carrier. It is worth noting that this thermodynamical expression of α is generally applicable and is also valid for materials with noticeable electronic correlations or in which conduction does not take place near the Fermi energy. Nevertheless microscopic models can be built, such as Mott's formula that accounts for the measured α [23]. This approach delivered good agreement with experimental results relating α to the electronic transport and magneto transport properties of some materials (see Ref. [24] and references therein).

3. Experimental results

The experiments were performed on a bulk polycrystalline sample of composition $(Fe_{0.96}Ni_{0.02})Rh_{1.02}$ cut in rod shape with rectangular cross section. A thin slice cut off the rod was used for C_p experiments. X-ray diffraction evidenced the well-ordered CsCl-type phase with the presence of the paramagnetic fcc phase. By means of scanning electron microscopy, the amount of the fcc phase was estimated to be approximately 6 vol%. Detailed description of the synthesis procedure can be found elsewhere [10]. Hall coefficient, magnetization, and α and C_p measurements under applied magnetic field were performed with Quantum Design Physical Property Measurement Systems.

Fig. 1 shows the low-temperature data for C_p, where the transition to the FM state at magnetic fields of 11 T and higher can be identified. An anomaly can be seen at the lowest temperatures, which in other magnetic systems was attributed to a gap Δ in the magnon spectrum [25]. For that reason, the magnetic contribution to C_p had the form $C_m = B_{FM}T^{3/2}e^{(-\Delta/T)}$ for the FM phase and $C_m = B_{AF}T^3 e^{(-\Delta/T)}$ for the AF phase [25]. The fitted values for γ were 62 ± 2 mJ kg^{-1} K^{-2} and 27 ± 1 mJ kg^{-1} K^{-2} for the FM and AF phases, respectively. Extrapolating the difference in γ to transition temperature, T_t, which at zero field is 256 K, results in an electronic entropy change $\Delta S_{el} = \Delta\gamma T_t = 8.9 \pm 0.2$ J kg^{-1}K^{-1}. This result is in good agreement with the value reported previously by Cooke et al. using different thin film proxies for the FM and AF phases of undoped FeRh [18].

In Fig. 2, the measured values of α are plotted, showing a jump and a change of sign at the expected transition temperatures. The shift in temperature of the jump is accompanied by an increased
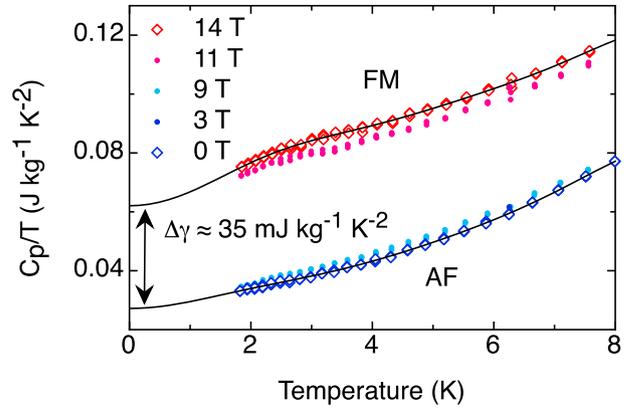

Fig. 1. Low-temperature heat capacity data for Ni-doped FeRh with different applied magnetic fields. At a field of 11 T and higher the system is in the FM state. Solid lines are fitted curves. FM, ferromagnetic; AF, antiferromagnetic.
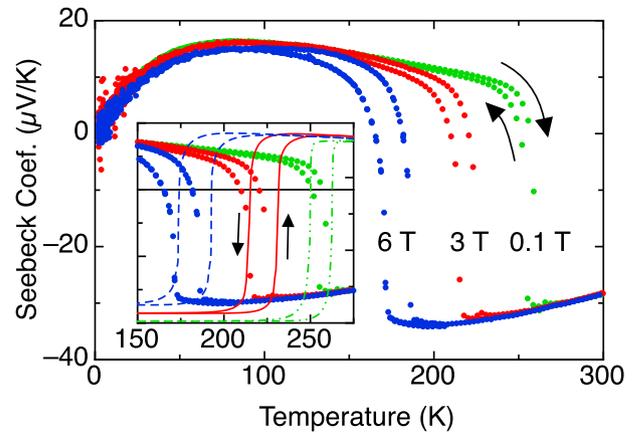

Fig. 2. Measured values of α acquired at different magnetic fields. Inset: Comparison of α with temperature-dependent magnetization curves measured in a different fragment of the same ingot (lines).

hysteresis in the AF region. In that region, the 6 T curve shows some slight deviation from the 0.1 and 3 T curves, which superimpose almost perfectly. In the FM phase, the heating and cooling curves superimpose perfectly within the experimental error of 2% for the three fields examined. Our data are in good agreement with the results obtained by Kobayashi et al. [26] in Ni-doped FeRh. In the FM phase, the applied magnetic field does not change the values of α. The displacement of the jump in α agrees with the one in magnetization (Fig. 2 inset). At higher fields and at temperatures lower than T_t, a residual non-zero magnetization is shown, indicating the presence of some ferromagnetically ordered part of the material.

Transverse resistance, R_{xy}, was measured as a function of applied magnetic field in one experiment up to 4 T and in a second experiment with a small applied field of up to 0.1 T. The temperature was changed with the sample in a demagnetized condition. Fig. 3a shows the transverse resistivity, ρ_{xy}, as a function of magnetic field for selected temperatures. The ordinary Hall coefficient r_h was obtained in the FM phase from the high field slope of the transverse resistivity curve [27]. A nearly constant r_h is obtained before and after the transition, with a jump and sign change in the transition region (Fig. 3b). The low value of r_h in the FM phase coincides with the observations of deVries et al. [29] in FeRh thin films and indicates the contribution of valence and conduction bands to the electronic transport, resulting in a situation close to
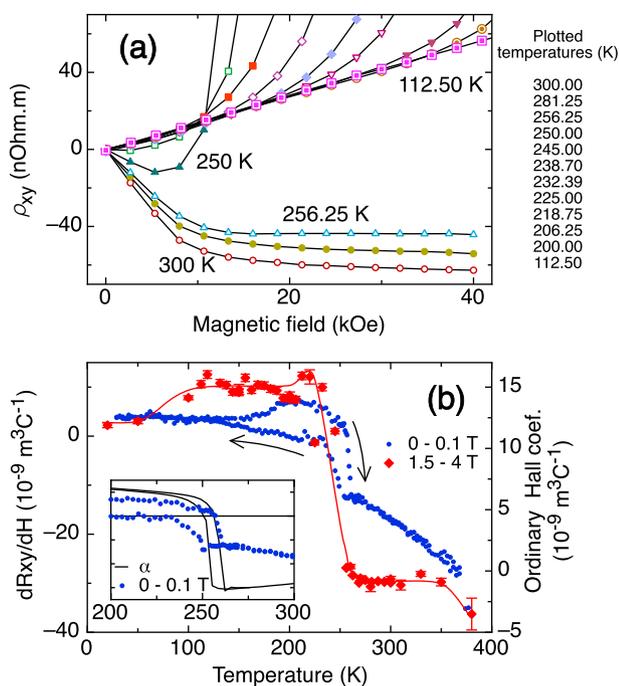
Fig. 3. (a) Transverse resistivity for selected temperatures. (b) dR_{xy}/dH measured at low fields and at magnetic saturation (ordinary Hall coefficient). Line is a guide to the eye. Inset: Detail of the low field dR_{xy}/dH and α at the transition region. Horizontal line is the zero level for both data sets.

compensation. In addition, r_h changes abruptly between 100 and 50 K, which might be related to a recently predicted martensitic transformation occurring at about 90 K [20]. The latter would need additional confirmation. For the AF phase, the slope of the R_{xy} curve was used before the FM state is induced by the strong field. Concerning the experiment at low field, the slope dR_{xy}/dH contains additional information about the initial susceptibility of the sample. In Fig. 3b, a significant contribution arising from the anomalous part of the Hall coefficient can be clearly identified for the high temperature FM phase. An approximately linear decrease of dR_{xy}/dH is observed as the temperature decreases towards the transition. A plateau is then observed at temperatures just above T_t both, on cooling and on heating. In addition, a complex hysteresis is seen in dR_{xy}/dH in the AF phase down to approx. 120 K, in contrast with the hysteresis observed in α, which shows no additional features in the AF region (Fig. 3 inset). Moreover, no hysteresis was evidenced in r_h in the temperature range 120−260 K.

Magnetization and transverse resistance point out that local FM spin arrangements occur in the AF phase. The dR_{xy}/dH indicate a complex magnetic interactions in the AF phase starting from 120 K until T_t. In this respect, it was recently shown that the presence of the fcc phase influences the transition temperature and hysteresis [28]. The actual way in which these possible local spin arrangements may be realized, the FM background seen in the AF phase, and the influence of the residual paramagnetic fcc phase present in the sample are subjects outside the scope of this article.

4. Discussion

According to the relation $\alpha = S_t/(eN_t)$, the effective transported charge needs to be known to extract the entropy information from the Seebeck coefficient. In the case of a single-band material, the extraction of the electronic entropy would be straightforward. In the present case, however, we have the contribution of two carrier

types in the FM phase. In the case of multiband conduction, r_h and α are typically regarded as conductivity weighted averages over the contributing bands, different for each coefficient [30]. According to the data in Fig. 3b, it is safe to use r_h to obtain a constant effective carrier concentration before and after the transition region. This allows for discussing the differences observed in the Seebeck coefficient in terms of differences in entropy production, although the numerical values may need a correction factor. The obtained values of ΔS_t increase from $\approx 3.7 \, J \, kg^{-1} K^{-1}$ at 0.1 T to $\approx 4.1 \, J \, kg^{-1} K^{-1}$ at 6 T (Fig. 4). This confirms that the contribution of the charge carriers to the entropy change is not constant. The applied magnetic field stabilizes the FM phase at lower temperatures, allowing α to continue its trend to increasingly negative values. This evidences an intrinsic shortcoming of the approach to characterize the entropy associated to the transported charge using C_p measurements at different magnetic fields or using proxies of different magnetically ordered states. The relative variation of the electronic entropy change with the applied magnetic field would then be of about 10% between zero and 6 T.

Note that in the FM state, the applied magnetic field does not change the value of α at a given temperature outside the transition region. Instead, the magnetic field keeps the material in the FM state until lower temperatures allowing α to monotonically become more negative. Consequently, an increase in entropy is evident in the FM phase when cooling down to T_t. The obtained ΔS_t increases with the applied magnetic field because α increases in the FM state at the corresponding T_t. In the AF phase, the variation of the entropy with temperature is rather small. However, some tendency to decrease the entropy with increasing temperature up to the transition may be noticed in the evolution of α and also in the increase of r_h (Fig. 3). This indicates that the difference in the electronic entropy between the AF and FM phases increases with approaching T_t from both sides. Such a behavior might be attributed to the enhancement of the spin fluctuation contribution in the d electron subsystem in the vicinity of the magnetic instability. In fact, the AF-FM transition in FeRh is accompanied by the changes in the Rh moment from zero up to approximately 1 μ_B, while the magnetic moment on Fe atoms does not remarkably vary (see Ref. [31] and references therein). Bearing that in mind, a spin-fluctuation contribution may be mainly associated with the Rh sublattice [32]. The role of spin fluctuations together with the difference in the density of electronic states with AF and FM order in the formation of properties of FeRh was recently demonstrated with first-principles calculations in the frame of the density functional theory [19].
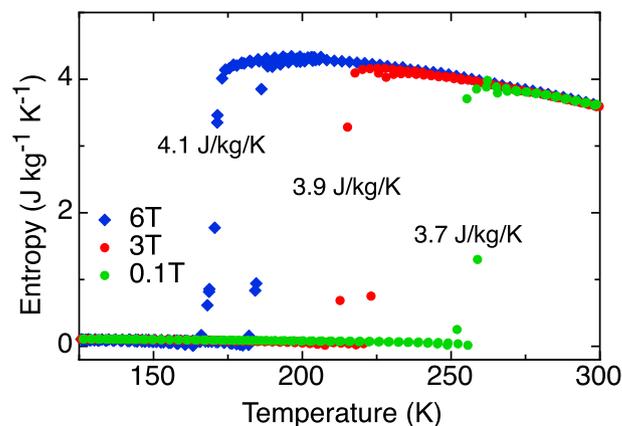

Fig. 4. Evolution of S_t with temperature for different magnetic fields.

5. Conclusions

The electronic entropy of a Ni-doped FeRh polycrystal was determined using low-temperature C_p measurements with applied magnetic fields. With the analysis of the Seebeck coefficient across the metamagnetic phase transition, we show that the entropy change associated with the conduction electrons is not constant. The applied magnetic field causes the electronic entropy change to increase up to 10% between 0.1 T and 6 T. This result sheds some light on the peculiar transition of FeRh alloys and can be of relevance in systems where free charge carriers are responsible for some key material properties like, in this case, itinerant magnetism.

Data availability

The raw/processed data required to reproduce these findings cannot be shared at this time because of technical or time limitations.

Conflict of interest

The author declares that they have no conflict of interest.

Acknowledgments

References

[1] F. Casanova, A. Labarta, X. Batlle, F. Perez-Reche, E. Vives, L. Manosa, A. Planes, Appl. Phys. Lett. 86 (2005) 262504.
[2] L. Manosa, D. Gonzalez-Alonso, A. Planes, E. Bonnot, M. Barrio, J.-L. Tamarit, S. Aksoy, M. Acet, Nat. Mater. 9 (2010) 478.
[3] G. Zhang, Z. Chen, B. Fan, J. Liu, M. Chen, M. Shen, P. Liu, Y. Zeng, S. Jiang, Q. Wang, Apl. Mater. 4 (2016), 064103.
[4] P.C. Canfield, S.L. Bud'ko, Rep. Prog. Phys. 79 (2016), 084506.
[5] Hagymasi2016I. Hagymasi, O. Legeza, Phys. Rev. B **93** (2016) 165104.
[6] Y.F. Lu, H. Kono, T.I. Larkin, A.W. Rost, T. Takayama, A.V. Boris, B. Keimer, H. Takagi, Nat. Commun. 8 (2017) 14408.
[7] J.E. Hirsch, Phys. Rev. B 95 (2017), 014503.
[8] V.M. Pudalov, A.Y. Kuntsevich, I.S. Burmistrov, M. Reznikov, J. Low Temp. Phys. 181 (2015) 99.
[9] P. Tu, A.J. Heeger, j.S.a. Kouvel, J. Appl. Phys. 40 (1969) 1368.
[10] N.V. Baranov, E.A. Barabanova, J. Alloy. Comp. 219 (1995) 139.
[11] K. Kreiner, H. Michor, G. Hilscher, N. Baranov, S. Zemlyanski, J. Magn. Magn. Mater. 177 (1998) 581.
[12] A. Chirkova, K.P. Skokov, L. Schultz, N.V. Baranov, O. Gutfleisch, T.G. Woodcock, Acta Mater. 106 (2016) 15.
[13] F. de Bergevin, L. Muldawer, C. R. Acad. Sci. 252 (1961) 1347.
[14] M.R. Ibarra, P.A. Algarabel, Phys. Rev. B 50 (1994) 4196.
[15] R.Y. Gu, V.P. Antropov, Phys. Rev. B 72 (2005), 012403.
[16] V.L. Moruzzi, P.M. Marcus, Phys. Rev. B 46 (1992) 2864.
[17] M. Wolloch, M.E. Gruner, W. Keune, P. Mohn, J. Redinger, F. Hofer, D. Suess, R. Podloucky, J. Landers, S. Salamon, F. Scheibel, D. Spoddig, R. Witte, B. Roldan Cuenya, O. Gutfleisch, M.Y. Hu, J. Zhao, T. Toellner, E.E. Alp, M. Siewert, P. Entel, R. Pentcheva, H. Wende, Phys. Rev. B 94 (2016) 174435.
[18] D.W. Cooke, F. Hellman, C. Baldasseroni, C. Bordel, S. Moyerman, E.E. Fullerton, Phys. Rev. Lett. 109 (2012) 255901.
[19] S. Mankovsky, S. Polesya, K. Chadova, H. Ebert, J.B. Staunton, T. Gruenbaum, M.A.W. Schoen, C.H. Back, X.Z. Chen, C. Song, Phys. Rev. B 95 (2017) 155139.
[20] N.A. Zarkevich, D.D. Johnson, Phys. Rev. B 97 (2018), 014202.
[21] A.F. Ioffe, Semiconductor Thermoelements and Thermoelectric Cooling, Infosearch Ltd., London, 1957.
[22] C. Goupil, W. Seifert, K. Zabrocki, E. Müller, G.J. Snyder, Entropy 13 (2011) 1481.
[23] N.F. Mott, Proc. R. Soc. London, Ser. A 156 (1936) 368.
[24] A. Frauen, A. Kobs, T. Böhnert, A.-K. Michel, G. Winkler, K. Nielsch, H.P. Oepen, Phys. Rev. B 92 (2015) 140402.
[25] J. Majzlan, J. Low Temp. Phys. 130 (2003) 69.
[26] Y. Kobayashi, K. Muta, K. Asai, J. Phys. Condens. Matter 13 (2001) 3335.
[27] N. Nagaosa, J. Sinova, S. Onoda, A.H. MacDonald, N.P. Ong, Rev. Mod. Phys. 82 (2010) 1593.
[28] A. Chirkova, F. Bittner, K. Nenkov, N. Baranov, L. Schultz, K. Nielsch, T. Woodcock, Acta Mater. 131 (2017) 31.
[29] M.A. de Vries, M. Loving, A.P. Mihai, L.H. Lewis, D. Heiman, C.H. Marrows, New J. Phys. 15 (2013).
[30] E.H. Putley, J. Phys. C Solid State Phys. 8 (1975) 3058.
[31] L.H. Lewis, C.H. Marrows, S. Langridge, J. Phys. D Appl. Phys. 49 (2016) 323002.
[32] G. Ju, J. Hohlfeld, B. Bergman, R.J.M. van de Veerdonk, O.N. Mryasov, J.-Y. Kim, X. Wu, D. Weller, B. Koopmans, Phys. Rev. Lett. 93 (2004) 197403.